

Density functional simulations of phase change materials: disordered phases of $\text{Ge}_8\text{Sb}_2\text{Te}_{11}$ and Ag/In/Sb/Te alloys

J. Akola^{1,2,3} and R. O. Jones¹

¹ Institut für Festkörperforschung, Forschungszentrum Jülich, D-52425 Jülich, Germany

² Nanoscience Center, Department of Physics, P.O. Box 35, FI-40014 University of Jyväskylä, Finland

³ Department of Physics, Tampere University of Technology, P.O. Box 692, FI-33101 Tampere, Finland

jaakko.akola@phys.jyu.fi r.jones@fz-juelich.de

ABSTRACT

Last year we described density functional simulations on the amorphous, liquid, and crystalline phases of GeTe, $\text{Ge}_{15}\text{Te}_{85}$, and $\text{Ge}_2\text{Sb}_2\text{Te}_5$ (GST-225, DVD-RAM) using large samples (up to 460 atoms in the unit cell) over hundreds of picoseconds. We found that atoms in these materials can be classified into atomic types A (Ge,Sb) and B (Te), with pronounced AB alternation, and the main structural motif is a four-membered ABAB ring (“ABAB square”). A considerable fraction of the Ge atoms have “tetrahedral” coordination (coexisting with “octahedral” coordination), the Sb and Te coordination numbers deviate from the “ $8-N$ rule” (N is the number of valence electrons), and small cavities (voids, vacancies) characterize these materials. The rapid amorphous-to-crystalline transition can be viewed as a re-orientation of distorted ABAB squares that is aided by the free space provided by the cavities. These calculations on massively-parallel IBM Blue Gene computers have been extended to other phase change alloys: $\text{Ge}_8\text{Sb}_2\text{Te}_{11}$, an alloy used in the Blu-ray Disc (BD), and $\text{Ag}_{3.5}\text{In}_{3.8}\text{Sb}_{75.0}\text{Te}_{17.7}$ (AIST). These represent two families used widely as phase change materials: pseudobinary alloys of the form $\text{GeTe}_{(1-x)}(\text{Sb}_2\text{Te}_3)_x$ ($x=1/3$ corresponds to $\text{Ge}_2\text{Sb}_2\text{Te}_5$) and doped Sb/Te alloys near the eutectic composition $\text{Sb}_{70}\text{Te}_{30}$, such as used in DVD-RW. We have performed a melt-quench simulation for $\text{Ge}_8\text{Sb}_2\text{Te}_{11}$ (GST-8,2,11, 630 atoms, over 400 ps), while AIST has been studied in its liquid phase (640 atoms, 850 K, 50 ps). The structures of amorphous (a-) GST-8,2,11 and GST-225 are similar, showing that adding a small amount of Sb changes the properties of GeTe significantly. GeTe differs from both GST-225 and GST-8,2,11 in its ring distribution, the increased number of Ge-Ge bonds, and its much lower cavity volume, but the differences between GST-8,2,11 and GST-225 are also significant. In particular, the latter has a larger Ge-Ge coordination number and more Ge atoms with tetrahedral coordination. The structure factor and pair distribution function of liquid AIST agree well with HEXRD measurements at 589°C (862 K). There is medium-range order, and Ag and In atoms (low-concentration “dopants”) prefer to be near Te atoms rather than Sb. Ag atoms are the most mobile, have the shortest bonds and highest coordination number, and are anionic. Indium is slightly cationic, and its bonds with Sb and Te are longer and more flexible than those of Ag.

Key words: Phase change materials, density functional calculations, molecular dynamics, $\text{Ge}_8\text{Sb}_2\text{Te}_{11}$, Ag/Sb/In/Te (AIST).

1. INTRODUCTION AND METHOD OF CALCULATION

Our focus remains the close and well-known relationship between the properties of a material and its atomic arrangement (“structure”), which is as valid in materials science as in other areas of physics, chemistry, and biology. Knowledge of the structures of the phases involved is essential to develop our understanding of the properties of *phase-change materials*, and theory has a decisive role to play. In principle, we need “only” to calculate the total energy of an aggregate of atoms for different atomic arrangements and temperatures and locate low-energy structures, but the practical problems are immense. Density functional (DF) calculations involve no adjustable parameters, and their predictive power in has been demonstrated in a wide range of contexts. The combination with molecular dynamics (the Car-Parrinello method [1]) has had a dramatic effect in materials science and chemistry, but the demands on computational resources are very large, and many simulations have been limited to systems with less than

100 atoms over some tens of picoseconds. These are profound restrictions for multi-element materials (which may also include cavities) where the time scale of the phase changes is longer than a nanosecond.

The present DF calculations were performed with the Car-Parrinello molecular dynamics package CPMD [2]. In contrast to our earlier work on GST-225, GeTe, and $\text{Ge}_{15}\text{Te}_{85}$ [3], where we used the generalized gradient approximation of Perdew, Burke and Ernzerhof (PBE) [4] for the exchange-correlation energy, we have used the PBEsol approximation [5] for GST-8,2,11 and Ag/In/Sb/Te, and the TPSS [6] approximation for elemental Te. We comment on the role of different functionals below. The electron-ion interaction has been described by ionic pseudopotentials with the form of Troullier and Martins [7]. The program employs periodic boundary conditions, usually with one point ($\mathbf{k}=0$) in the Brillouin zone, and we used 20 Ry for the kinetic energy cutoff of the plane wave basis in GST-8,2,11. These simulations used 630 atoms (240 Ge, 60 Sb, 330 Te) in a cubic cell of dimension (27.19 \AA) appropriate to the liquid density ($0.03134 \text{ atoms/\AA}^3$). The starting geometry was based in part on our optimized geometry for GST-225 (460 atoms). After heating to 3000 K, the sample was cooled (over 120 ps) to the melting point (950 K), where data were collected (31 ps). During further cooling to 300 K (217 ps), there was a small adjustment of the density to that of the amorphous material ($0.03179 \text{ atoms/\AA}^3$). This was followed by data collection (30 ps) and cooling to 100 K, where the structure was optimized by simulated annealing. The total simulation time was 429 ps, and more details are given in Ref. [8].

The simulations of liquid AIST used 640 atoms (23 Ag, 25 In, 480 Sb, 112 Te) distributed initially in a cubic cell (size 27.087 \AA) appropriate to the density of the liquid ($0.03220 \text{ atoms/\AA}^3$). The kinetic energy cutoff of the plane wave basis set (60 Ry) is much higher than in GST systems, because the 4d levels in Ag and In must be included in the “valence” configuration. The simulation was started at 3000 K, followed by cooling to 850 K (30 ps, time step 4.8 fs) and data collection (20 ps, time step 3.0 fs). Full details are provided elsewhere [9].

The use of Born-Oppenheimer MD, where the orbital eigenfunctions are optimized for each ionic configuration, has been essential to the present work. In particular, it allows much longer time steps than in standard Car-Parrinello calculations and is stable for systems with small or vanishing band gaps. MD methods allow us to follow the coordinates R_i and velocities v_i of all atoms i throughout the simulations, leading to pair correlation functions $g_{ij}(r)$ for pairs of atom types i, j . An appropriate Fourier transformation yields the structure factor $S(Q)$. Insight into the local order can be found from the distributions of the bond and dihedral angles and by defining order parameters similar to those used in the theory of binary liquids [3]. For discussion purposes it is convenient to separate atoms into types A (Ge, Sb) and B (Te).

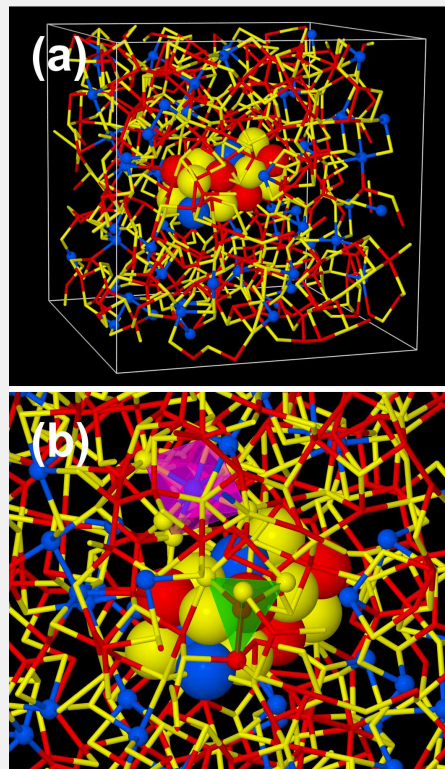


Figure 1. Simulation of GST-8,2,11: (a) Simulation box (630 atoms). A “column” with AB ordering is shown, and Sb atoms are shown as small spheres. Red: Ge, yellow: Te, blue: Sb. (b) Structures with tetrahedrally coordinated Ge atom (green) and octahedrally coordinated Sb (pink).

3. RESULTS AND DISCUSSION

A. $\text{Ge}_8\text{Sb}_2\text{Te}_{11}$ (GST-8,2,11)

The optimized structure of a-GST-8,2,11 (Figure 1) leads to the pair distribution function (PDF) shown in Figure 2(b). In the absence of published scattering data on this system, we compare our calculated structure factor $S(Q)$ [Figure 2(a)] with measurements on GeTe and GST-225 [9]. It may be surprising that the results for GST-8,2,11 appear closer to those for GST-225 than those for GeTe, but this impression is supported by the partial PDF in Figure 3. Ge-Te and Sb-Te bonds dominate, with partial coordination numbers 3.2 and 2.8, respectively, and the Te-Te PDF shows medium range oscillations extending beyond 10 Å. The number of “wrong bonds”, i.e. those not occurring in the crystal, is much lower in the sample at 300 K. The PBEsol approximation reduces bond lengths by 1-2 %. In GST-225, this results in improved agreement with EXAFS measurements [3]. In GST-8,2,11, both Sb and Te have higher coordination than expected from the “8- N rule”, where N is the number of valence electrons. Sb atoms show interesting points of similarity to other GST alloys, and we provide more information on this as and the distributions of bond and dihedral angles in Ref. [8]. The dihedral distributions are interesting, since Ge shows some preference for octahedral configurations, but the distribution for Sb is definitely octahedral, with pronounced maxima at 0 and 90°.

The ring statistics of amorphous GST-8,2,11, GeTe, and GST-225 are compared in Figure 4. In all cases there are many four-membered rings and few triangular configurations. As in GST-225, most of the four-membered rings in GST-8,2,11 show AB alternation, indicating that the basic building blocks in the amorphous and crystalline (rocksalt) phases are “ABAB squares”. An example is the “ABAB column” in Figure 1(a). The odd-even alternation is apparent in both GST-8,2,11 and GST-225, and the ring distributions of these two materials are strikingly similar. This may be surprising, since GST-8,2,11 ($x=1/9$) is closer on the pseudobinary line $\text{GeTe}_{(1-x)}(\text{Sb}_2\text{Te}_3)_x$ to GeTe ($x=0$) than to GST-225 ($x=1/3$). It is clear that even small amounts of Sb change the properties of GeTe significantly.

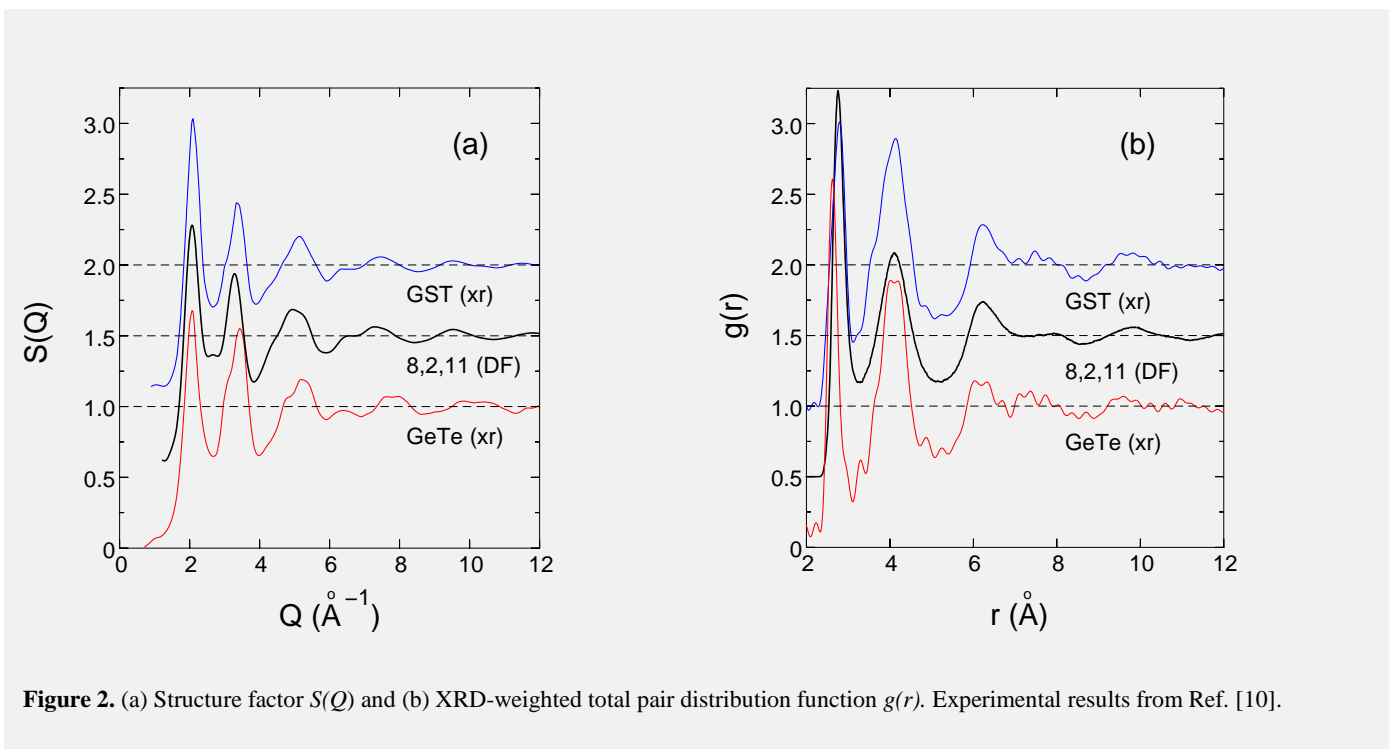


Figure 2. (a) Structure factor $S(Q)$ and (b) XRD-weighted total pair distribution function $g(r)$. Experimental results from Ref. [10].

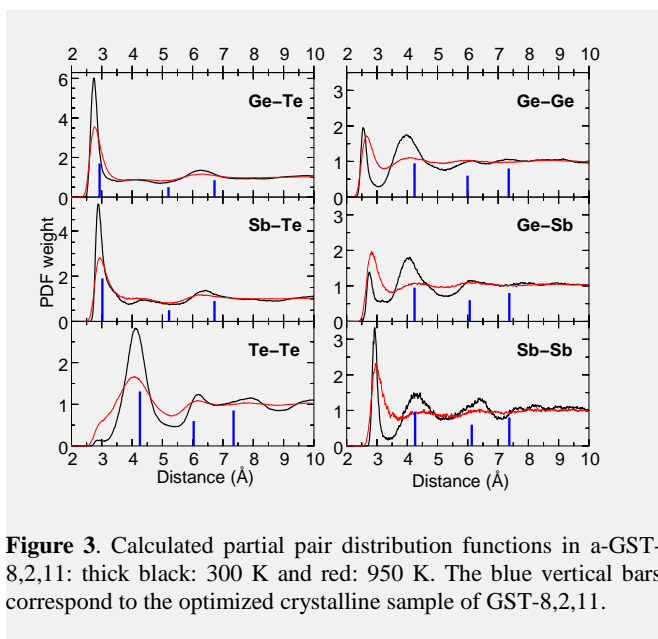


Figure 3. Calculated partial pair distribution functions in a-GST-8,2,11: thick black: 300 K and red: 950 K. The blue vertical bars correspond to the optimized crystalline sample of GST-8,2,11.

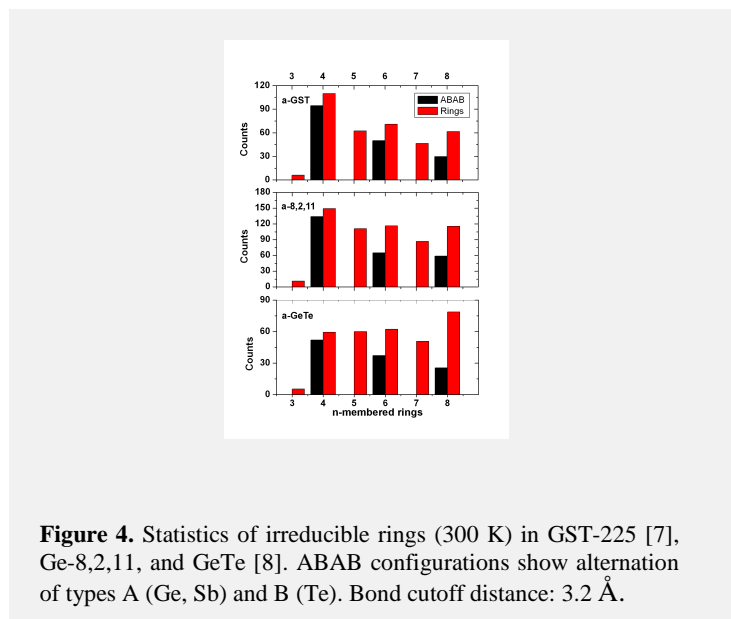


Figure 4. Statistics of irreducible rings (300 K) in GST-225 [7], Ge-8,2,11, and GeTe [8]. ABAB configurations show alternation of types A (Ge, Sb) and B (Te). Bond cutoff distance: 3.2 Å.

Our earlier work [3] has shown that cavities play an essential role in Ge/Sb/Te alloys. Crystalline GST-225, for example, contains 10% vacancies. The amorphous form, whose density is 7% lower, will contain empty regions, and we showed that they comprise 11.8 % of the total volume of a-GST (slightly more than in the crystal), increasing to 13.8 % at 900 K [3]. These values are larger than in a-GeTe (6.4 %) and consistent with the better performance of GST-225 as a phase change material. The situation in the optimized structure of a-GST-8,2,11 is shown in Figure 5, where cavities form facets, edges, corners, and protrusions and occupy 12.4 % of the total volume, i.e. the addition of a small amount of Sb is accompanied by a dramatic increase in the number of cavities to a value near that in a-GST-225. The coordination numbers around the vacancy centres are 1.3, 0.4, 3.7, and 0.2 for Ge, Sb, Te, and other vacancies, respectively. The cavities are then surrounded mainly by Te atoms, and Ge is a more common neighbour than Sb. The average vacancy in the crystalline phase contains 1.6 electrons, close to the amorphous value. The larger volume fraction (19.3%) occupied by cavities in liquid GST-8,2,11 (950 K) is consistent with the increased coordination number of Ge (4.3) and the lower density.

The electronic structure resulting from the DF calculations can be compared with the results of XPS measurements. We report full details in Ref. [8], where we also discuss dynamical properties (power spectra, diffusion constants, etc.) that can be determined from the MD trajectories. The vibration frequencies provide important structural information, and more such measurements for phase-change materials would be very welcome.

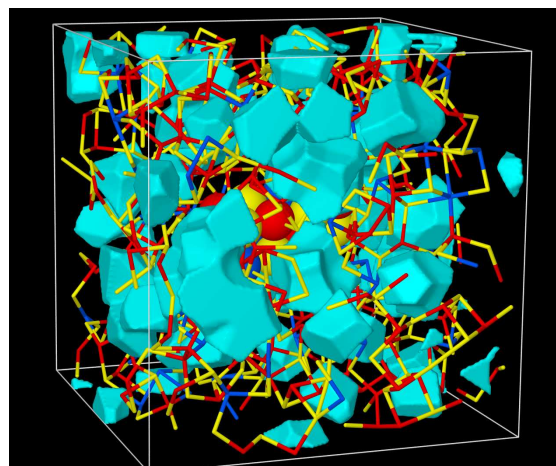


Figure 5. Cavities in melt-quenched GST-8,2,11. The blue surfaces enclose regions at least 2.8 Å from any atom.

B. $\text{Ag}_{3.5}\text{In}_{3.8}\text{Sb}_{75.0}\text{Te}_{17.7}$ (AIST).

The snapshot of liquid AIST in Figure 6 emphasizes small cavities and the sparsely distributed (dopant) atoms Ag and In. On average there are only 22 cavities in the 640 atom sample, and their total volume ($\sim 4\%$) is much less than in liquid GST-225 ($\sim 14\%$) or its amorphous form ($\sim 12\%$), where they are crucial to the phase change mechanism.

The calculated structure factor $S(Q)$ and the total pair distribution function $g(r)$ were determined from 13 snapshots of structures taken at 850 K and are shown in Figure 7. The agreement between theory and experiment is very good for both $S(Q)$ [Figure 7(a)] and $g(r)$ [Figure 7(b)], although the minor deviations in the latter near the first peak and the weak second maximum at 4.2 \AA suggest that the calculated coordination numbers might be slightly larger than the experimental estimates. Seven partial PDF are shown in Figure 8. As in liquid GST-225, there are signs of medium-range order and few Te-Te contacts. Bonds between In and Sb/Te are longer (by $0.2 - 0.3\text{ \AA}$) than bonds between Ag and Sb/Te, and both Ag and In prefer Te neighbours over Sb. The total coordination numbers [8] indicate that Ag and In increase the overall coordination, and they tend to form bond angles near 90 degrees when associated with Te. As in the case of GST-8,2,11, we have calculated the electronic structure of liquid AIST as well as dynamical properties (power spectrum and diffusion constants), and more information is provided in Ref. [8]. Ag atoms are the most mobile, and the main structure in the vibrational density of states is a broad peak near 100 cm^{-1} arising from Sb vibrations.

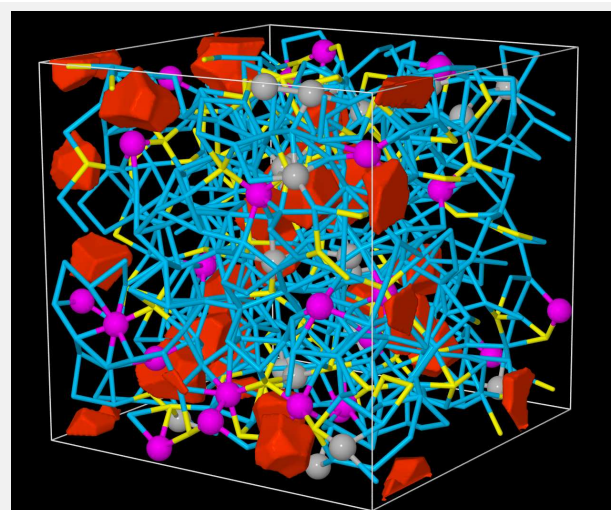


Figure 6. Snapshot of l-AIST (Ag: silver, In: magenta, Sb: blue, and Te: yellow). The dopants (Ag, In) are depicted with small spheres, the cavities are shown in red.

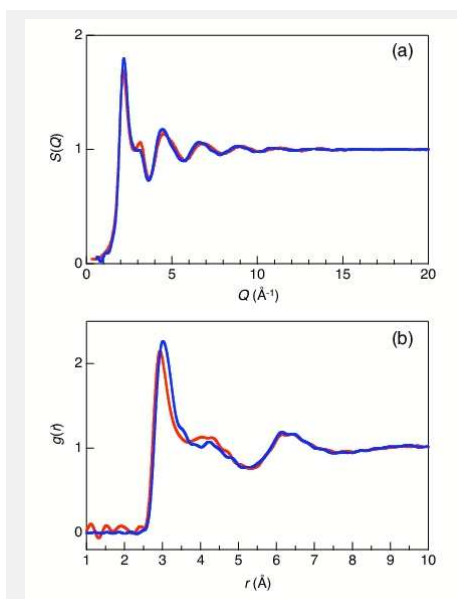


Figure 7. (a) Structure factor $S(Q)$ in AIST (850 K), (b) Total PDF $g(r)$ with XRD weights. Red: XRD (862 K) with $Q_{\text{max}}=25\text{ \AA}^{-1}$ in Fourier transform, blue: present simulation.

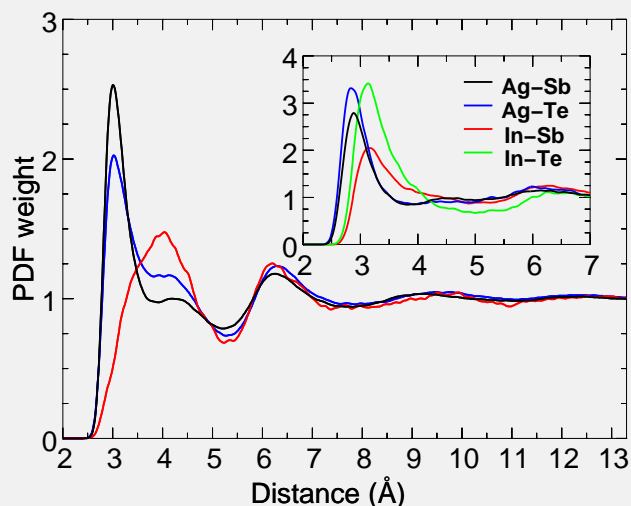


Figure 8. Partial RDF in AIST at 850 K. Black: Sb-Sb, blue: Sb-Te, red: Te-Te. Inset: Ag-Sb, Ag-Te, In-Sb, and In-Te.

4. CONCLUDING REMARKS

We have summarized here results of massively parallel simulations (IBM Blue Gene computers) on $\text{Ge}_8\text{Sb}_2\text{Te}_{11}$ (GST-8,2,11) and $\text{Ag}_{3.5}\text{In}_{3.8}\text{Sb}_{75.0}\text{Te}_{17.7}$ (AIST). The availability of computers of this (“capability”) class and the development of efficient algorithms have made DF calculations possible for systems with hundreds of atoms over time scales of hundreds of picoseconds, i.e. approaching the crystallization time of phase change materials. Not only has this enabled us to identify the crucial pattern (“ABAB squares”) in the structural phase transition in $\text{GeTe-Sb}_2\text{Te}_3$ pseudobinary alloys, but it has brought to light surprising similarities between the structures of GST-225 and GST-8,2,11, although the *composition* of the latter is much closer to GeTe. The properties of GeTe are changed dramatically by adding a small amount of Sb. We are certain that MD/DF calculations will continue to provide insight into materials of interest to the phase-change community.

We close, however, with words of caution similar to those of last year. First, these calculations and their analysis are immensely demanding of both computing resources *and* manpower, and their application to alloys with several elements and complicated compositions cannot be viewed as “routine”. Small simulation cells simply cannot provide evidence for the existence or otherwise of medium-ranged order, and this is also true for studies of cavities, which can occur as multivacancies in these systems. It is also crucial that the cooling time for the liquid be close to that of the physical processes involved, since rapid quenching leads invariably to artificially high numbers of “wrong bonds”. The use of Born-Oppenheimer MD with an efficient predictor-corrector scheme for converging the orbital eigenfunctions has been decisive in this work. The time steps are two orders of magnitude greater than in Car-Parrinello simulations of other systems, and this is aided by the high atomic numbers of the component elements. Finally, high temperatures favour metallic samples in these systems, and the absence of a gap in the eigenvalue spectrum often leads to instabilities in the Car-Parrinello approach.

Work continues on these and other projects. Of particular interest to many researchers is elemental Te, for which experimental and calculated structure factors and pair distribution functions often disagree. We have noted above the differences that can be found with DF simulations that use different functionals, and this is certainly the case in Te. Present indications are that the TPSS functional [6] gives the best agreement between experiment and theory, but we note that this functional goes beyond gradient corrections and is even more demanding of computer resources than gradient expansions such as PBE [4] and PBEsol [5].

The calculations were performed on IBM Blue Gene/L, Blue Gene/P, and p6 575 computers in the Forschungszentrum Jülich with grants from the FZ Jülich and the John von Neumann Institute for Computing. We thank S. Kohara, T. Usuki, K. Kobayashi, T. Matsunaga, and N. Yamada for helpful discussions and providing original data, and P. Westpfahl for help in the battle with Microsoft Word®.

REFERENCES

1. R. Car and M. Parrinello, “Unified approach for molecular dynamics and density functional theory”, Phys. Rev. Lett. **55** (1985) 2471.
2. CPMD V3.12: © IBM Corporation 1990-2008; © MPI für Festkörperforschung, Stuttgart 1997-2001 (<http://www.cpmid.org>).
3. J. Akola and R. O. Jones, “Structural phase transitions on the nanoscale: The crucial pattern in the phase change materials $\text{Ge}_2\text{Sb}_2\text{Te}_5$ and GeTe”, Phys. Rev. B **76** (2007) 235201; “Binary alloys of Ge and Te: order, voids, and the eutectic composition”, Phys. Rev. Lett. **100** (2008) 205502; “Density functional study of

- amorphous, liquid and crystalline $\text{Ge}_2\text{Sb}_2\text{Te}_5$: Homopolar bonds and/or AB alternation?" *J. Phys. Condens. Matter* **20** (2008) 465103.
4. J. P. Perdew, K. Burke, and M. Ernzerhof, "Generalized gradient approximation made simple", *Phys. Rev. Lett.* **77** (1996) 3865.
 5. J. P. Perdew, A. Ruzsinszky, G. I. Csonka, O. A. Vydrov, G. E. Scuseria, L. A. Constantin, X. Zhao, and K. Burke, "Restoring the density-gradient expansion for exchange in solids and surfaces", *Phys. Rev. Lett.* **100** (2008) 136406.
 6. J. Tao, J. P. Perdew, V. N. Staroverov, and G. E. Scuseria, "Climbing the density functional ladder: Non-empirical meta-generalized gradient approximation designed for molecules and surfaces", *Phys. Rev. Lett.* **91** (2003) 146401.
 7. N. Troullier and J. L. Martins, "Efficient pseudopotentials for plane-wave calculations", *Phys. Rev. B* **43** (1991) 1993.
 8. J. Akola and R. O. Jones, "Structure of amorphous $\text{Ge}_8\text{Sb}_2\text{Te}_{11}$: $\text{GeTe-Sb}_2\text{Te}_3$ alloys and optical storage", *Phys. Rev. B* **79** (2009) 134118.
 9. J. Akola and R. O. Jones, "Structure of liquid phase change material AgInSbTe from density functional/molecular dynamics simulations", *Appl. Phys. Lett.* **94** (2009) 251905.
 10. S. Kohara, K. Kato, S. Kimura, H. Tanaka, T. Usuki, K. Suzuya, H. Tanaka, Y. Moritomo, Matsunaga, N. Yamada, Y. Tanaka, H. Suematsu, and M. Takata, "Structural basis for the fast phase change on $\text{Ge}_2\text{Sb}_2\text{Te}_5$: Ring statistics analogy between the crystal and amorphous states", *Appl. Phys. Lett.* **89** (2006) 201910.

Biographies

J. Akola studied Physics at the Universities of Helsinki and Jyväskylä, Finland, obtaining his Ph.D. at Jyväskylä under Matti Manninen. After five years as a Post-doctoral Researcher at the Forschungszentrum Jülich, Germany, he returned in 2005 to the Nanoscience Center in Jyväskylä. Since 2008, he is also at Department of Physics, Tampere University of Technology. His fields of interest include classical, tight-binding, and density functional simulations of materials, nanoparticles, and biological systems.

R. O. Jones obtained his B.Sc. Hons (Physics) at the University of Western Australia in Perth and his Ph.D. at the University of Cambridge, England under Volker Heine. He spent three years as a Post-doctoral Associate at Cornell University before joining the FZ Jülich. His main focus for over 30 years has been on density functional theory and its applications to a wide range of ordered and disordered systems (solids, surfaces, atomic clusters, molecules, polymers, biological molecules, ...).